Influences of Crystallization Histories on PTC/NTC Effects of PVDF/CB Composites

MINGYIN ZHANG,* WENTAO JIA, and XINFANG CHEN

Department of Materials Science, Jilin University, Changchun 130023, People's Republic of China

SYNOPSIS

Two switching phenomena of poly(vinylidene fluoride) (PVDF) containing carbon black (CB) with different crystallization histories are studied. Both the percolation threshold (Φpc) and the critical concentration of the positive temperature coefficient (PTC) materials (Φc) increase as the crystallization temperature declines. PTC and the negative temperature coefficient (NTC) effect become obvious when the cooling speed is reduced. The morphologies of PVDF crystals play an important role in modifying the shape of the resistivity–temperature (ρ–T) curves. The PTC and NTC intensities of these systems, whose CB contents lie between Φpc and Φc, increase with increasing crystallinity, which are realized by altering the crystallization histories of the matrices. © 1996 John Wiley & Sons, Inc.

INTRODUCTION

There are two switching phenomena in crystalline polymers filled with conductive particles. The first one is called the percolation transition. The conductivity of the composite increases slowly as the content of the filler increases, and then there is a sudden increase of some 10 orders of magnitude or even more in the conductivity when the filler content reaches a certain level (percolation threshold [Φpc]), after which the conductivity increases slightly and monotonically as the filler is added further.

The first switching phenomenon is regarded as a geometric phase transition.[1-6] Experimental[1,6] as well as theoretical[2-6] studies of the percolation phenomenon have been reported.

The second switching phenomenon is also called the positive temperature coefficient (PTC) effect, i.e., the resistivity of the composite increases remarkably as the elevated temperature reaches the vicinity of the melting point of the polymer matrix, and is then followed by the negative temperature coefficient (NTC) effect by which the resistivity declines quickly beyond the critical temperature (T_c), which is determined by the melting point of the crystalline polymer.[7-14]

It has been found that the maximum PTC intensity appears at the critical carbon black (CB) concentration (named Φc), which is slightly larger than the percolation threshold (Φpc)[9,11] that is determined by the conductivity of CB and the polymer species.[15,16] Narkis et al.[9] and Sircar and Wells[17] showed that any CB parameter which increases conductivity (loading, surface area, structure, porosity) decreases Φpc, Φc, the PTC effect, and the width of PTC intensity–Φ curve.

In early works, there are many studies on the PTC/NTC effects of PE/CB composites[8,11-13] and several theories about PTC/NTC effects on the basis of the system[7,14,18] have been established. In this article, the effects of the crystallization histories on Φpc and Φc, ρ–T plots, and PTC and NTC intensities are reported. Wide-angle X-ray diffraction (WAXD) and differential scanning calorimetry (DSC) are used to illustrate the effects of the morphologies of poly(vinylidene fluoride) crystals on the resistance behaviors of the composites which have undergone increasing temperature. All the results give new evidence on the model that the CB aggregates distribute around the crystalline regions in semicrystalline polymer and the nonequilibrium thermodynamical model for the NTC effect.

EXPERIMENTAL

Composite Samples Preparation

Poly(vinylidene fluoride) (PVDF) was obtained from U.S.A. Pennwalt Co.; the commercial identification

* To whom correspondence should be addressed.

Journal of Applied Polymer Science, Vol. 62, 743–747 (1996)
 CCC 0021-8995/96/050743-05

Table I Crystallization Histories the Samples

Cooled Method	Definitions of the Methods
Cooled slowly	Cooled under pressure from 200°C to room temperature
Air cooling	Cooled in air from 200°C to room temperature
Quenched	Cooled from 200°C in water with different temperature

was N460, its melting range was from 160 to 170°C, and density was 1.76 g/cm^3. Carbon black (CB) was CSF3 type, produced by the Changchun Institute of Applied Chemistry, China. The average size of aggregates was 70 nm; surface area, 230 m^2/g; DBP value, 280 mL/100 g; and PH value, 7–9.

PVDF and CB with different proportions were mixed in Brabender for 5 min at 200°C, then kneaded on two-roll mill for 5 min at 190°C. The composites were compression-molded at 200°C for 10 min, then cooled by several methods (see Table I). The sheets are 1 mm thick.

Resistivity Measurements

The volume resistivity was measured with a two-electrode system and copper foils were adhered on both sides of the sheet to eliminate the contact resistance. A programmed temperature controller was used to heat the electrodes at the speed of 5°C/min. The lower resistances (<20 MΩ) were measured by a digital multimeter. An insulating tester was used to measure the higher resistances (≥20 MΩ).

Characterization

Wide-angle X-ray diffraction was obtained by a rotating Cu-anode X-ray source. The mean dimensions of the crystallites perpendicular to the plane (110) were calculated by the Scherrer equation:

$$L_{hkl} = \frac{K\lambda}{\beta_{1/2} \cos \theta} \quad (1)$$

where $\beta_{1/2}$ is the half-width of the maximum intensity of the pure diffraction profile in radians; λ, the X-ray wavelength; K, equal to 0.9 for our calculation; and θ, the Bragg angle.

The thermoanalysis was carried out with a Perkin-Elmer differential scanning calorimeter (DSC-7) and the enthaply of fusion, ΔH_f, was obtained. We took ΔH_f^0 = 104.7 J/g (ref. 19) as the enthaply of fusion for the 100% crystalline sample. Then, the crystallinity was calculated by the expression

$$X_c = \frac{\Delta H_f}{\Delta H_f^0} \times 100\% \quad (2)$$

RESULTS AND DISCUSSION

Effect of the Crystallization Histories on the Critical Values

In these random and macroscopically homogeneous polymer/CB materials, it has been demonstrated that at the content of the filler below the Φ*pc* (Φ < Φ*pc*) a short-range percolation coherence length,[6] ζ, exists, conduction only occurring within domains which are smaller than ζ. As the content of the filler approaches Φ*pc*, ζ increases infinitely (ζ → ∞), i.e., the infinitely conductive network[3] comes into being and the composite becomes isotropically conductive.

In Figure 1, curves (a) and (b) show the resistivities as functions of CB content and the crystallization histories. The entire region of the decrease in resistivity [e.g., region B in curve (b)] is called the percolation region.[20] The content at the end of this region is defined as the critical content of PTC materials (Φ*c*). Both Φ*pc* and Φ*c* increase as the cooling speed accelerates. The Φ*pc* and Φ*c* are 7 and 11 wt % for the slowly cooled sample and 8 and 13 wt % for air-cooled sample, respectively.

It is well known that the CBs prefer to disperse in the amorphous regions of the semicrystalline polymer; therefore, the critical values decrease as the degree of the crystallinity increases.[11] According to the DSC results, the percent crystallinities of pure PVDF are 49 and 46% for slowly cooled and air-

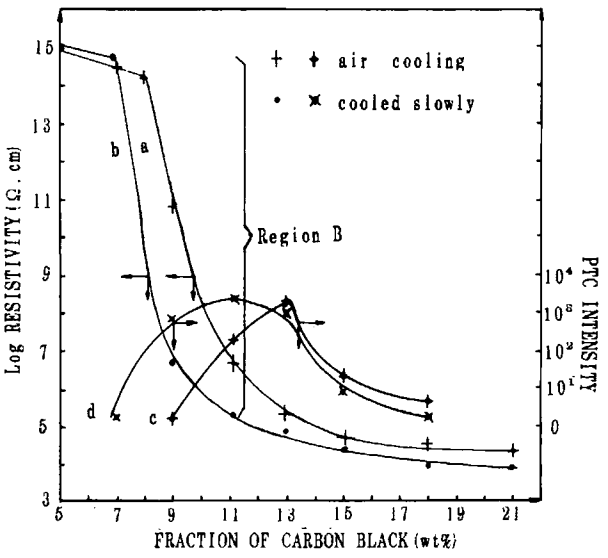

Figure 1 ρ–Φ and PTC intensity–Φ plots of PVDF/CB composites.

cooled samples, respectively. The volume of the amorphous regions of the sample which was cooled slowly is smaller than that of the air-cooled one, so the effective content of CBs of the former is larger than that of the latter, for given amounts of CBs.

Effect of the Crystallization Histories on the PTC/NTC Behaviors

The ρ–T plots of PVDF/CB composites characterized by different crystallization histories is shown in Figure 2. It can be seen that, with the decreasing crystallization temperature the peak of the ρ–T curve shifts to low temperature ($T_c^c < T_c^b < T_c^a$), and the width of the peak becomes large. The room-temperature resistivity increases as the cooling speed becomes fast. This is probably due to the variation of the crystallinity of the matrix, as is discussed in the preceding subsection. The samples quenched in water show an obvious PTC effect even at the lower temperature. At the same time, the transition temperature (T_t) (intersection of the tangent to the point of inflection of the ρ–T curve with the horizontal from ρ_{room})[8] shifts to a lower temperature as the sample is cooled quickly.

Figure 3 shows DSC measurements for pure PVDF with different crystallization histories. It can be seen that there are two melting peaks in curves (b) and (c): a low-temperature peak and a high-temperature peak. The two peaks combine into one high-temperature peak when the sample is cooled slowly [curve (a)]. One can also find that the width of the DSC peak of the sample with the lower crystallization temperature is larger than that of the sample with the higher crystallization temperature, i.e., the

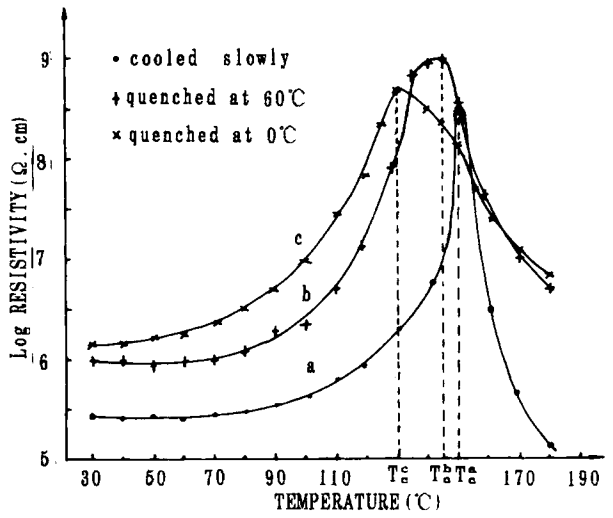

Figure 2 ρ–T plots for CB-filled PVDF composites with different crystallization histories.

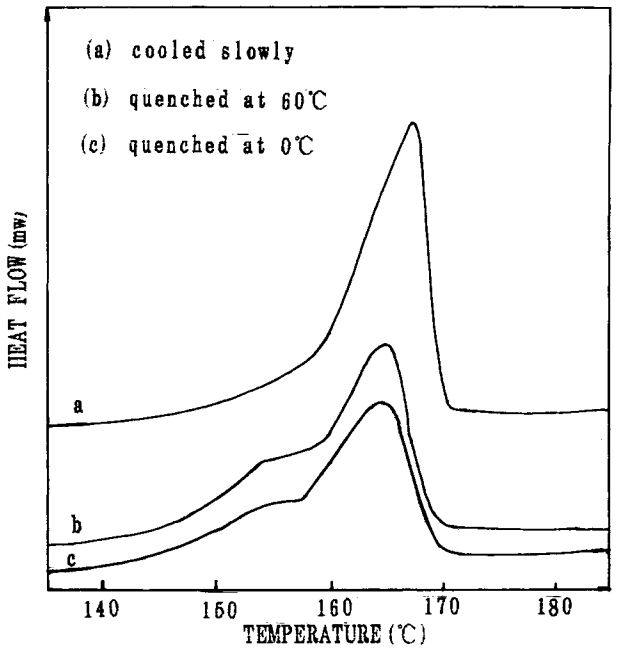

Figure 3 DSC thermograms of pure PVDF with different crystallization histories.

melting temperature (T_m) decreases and the melting range increases as the sample is cooled quickly.

If the polymer is quenched from the melt to a temperature greatly below the T_m, both the crystal growth rate and nucleation rate will be rather large.[21] Many nuclei growing simultaneously will result in great interference between the various crystallites. The size of the crystallites will be decreased, since their volume of growth is restricted by the surrounding crystallites. Furthermore, it is probable that the region of contact between growing centers will result in a poorly ordered, strained, or perhaps even an amorphous region. Both of these factors will cause the resulting crystals to be unstable at temperatures greatly below T_m. If the crystalline sample is warmed very slowly, the small imperfect crystals melt at lower temperatures but then recrystallize into more perfect forms. The bipeak phenomenon contributes to the melting–recrystallizing process (see Fig. 3).

If the sample is crystallized very slowly, crystals must have extraordinary perfection and size. Since the growth occurs very slowly, a great opportunity exists for defects in the structure to be eliminated by alternate "melting" and "freezing" of a chain as it is added to the crystal growth surface. On the other hand, since the number of nuclei would be very small in this temperature range, each nucleus can grow into very large crystallites before encountering interference from other growing nuclei. As a result of the high perfection and large size, the crys-

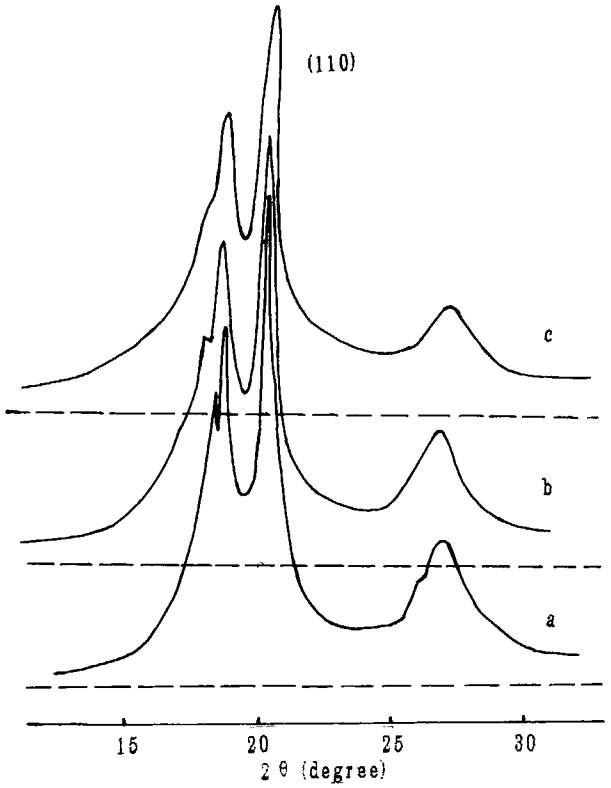

Figure 4 X-ray diffractograms of pure PVDF crystallized from the melt. (Curves a, b, and c are the same as in Fig. 3.)

tallites thus formed nearly have the melting point of a perfect crystal (T_m). Therefore, the melting curve of the slowly cooled sample has only one high-temperature peak.

Thus, in Figure 2, the enhancement of the PTC effect at lower temperature and decreases in T_c and T_t of the sample which was crystallized at very low temperature are attributed to the melting–recrystallizing of imperfect and small crystallites. The change in resistance with increasing temperature takes place at the start of the low-temperature peak of DSC and is kept until the high-temperature peak. So, the ρ–T curve is much broader. For the slowly cooled sample, its perfect and large crystallites will not melt until the temperature is elevated to the vicinity of the high-temperature peak of DSC. So, the resistance will initially hardly change until the temperature reaches T_t. The anomaly only exists within a narrow range of temperature.

The WAXD results of the samples are shown in Figure 4. The half-width of the maximum intensity of the pure diffraction profile becomes wide as the crystallizing speed is quickened. The half-width in degrees and the mean dimensions of the crystallites perpendicular to the plane (110) are calculated by eq. (1). The results are shown in Table II. The large half-width and the small mean dimension illustrate that the dimensions of the crystallites are distributed broadly when the sample is cooled quickly, i.e., there exist imperfect and small crystallites. When the sample is cooled slowly, small crystallites are few and most crystallites are relatively complete. These results are consistent with those of the DSC discussed above.

The NTC effects of the samples are enhanced as the crystallizing temperature increases, which are also shown in Figure 2. As we know, energy is given to CBs by the advancing crystallite fronts as the crystalline regions are melting. Meanwhile, the shear modulus decreases remarkably when the crystalline regions begin to melt.[11] In addition, the interfacial excess energy of the real composite is in a nonequilibrium state and can increase with time for a given CB amount.[8] Then, more energy will be obtained by CBs when the sample is cooled more slowly. The higher the Gibbs' free energies obtained by CBs,[22] the easier the CBs flocculate and phases of the composite separate and the more obvious the NTC effect is.

Effect of the Crystallization Histories on the PTC/NTC Intensities

The effects of most parameters of the matrix, such as peak melting point, melting range, expansion coefficient, and the heat of fusion on PTC intensity, have no universal laws, but the large crystallinity and low T_g do enhance the PTC intensity.[8] The effect of crystallinity on PTC and NTC intensities is discussed below. The PTC intensity refers to the ratio of the peak resistivity to the resistivity at room temperature (ρ_{peak}/ρ_{room}) and NTC intensity refers to the ratio of the peak resistivity to the resistivity at 180°C for the PVDF/CB system ($\rho_{peak}/\rho_{180°C}$).[23]

The PTC intensities, as functions of CB contents and the crystallization histories are shown in Figure 1. The two samples that are cooled slowly [curve (c)] and cooled in air [curve (d)], respectively, show the similar result that the maximum PTC intensity oc-

Table II Half-width and the Mean Dimension of the Crystallites Perpendicular to Plane (110)

Cooling Method	Half-width	Mean Dimension of the Crystallites (μm)
Cooled slowly	0.36°	22.4
Air cooling	0.40°	20.1
Quenched	0.50°	16.2

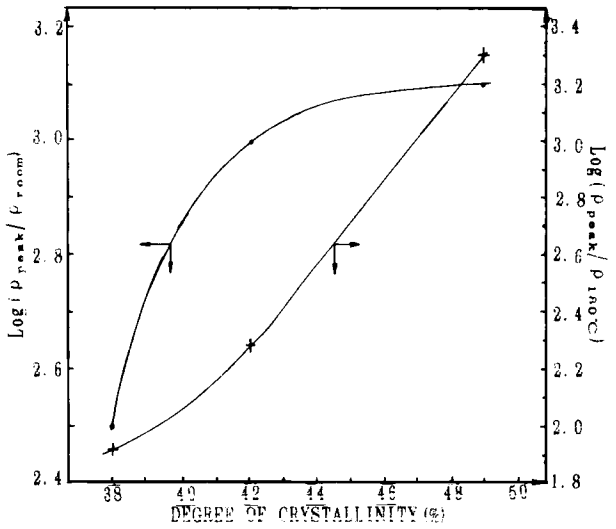

Figure 5 Plots of the PTC and NTC intensities against the crystallinity of the PVDF.

curs at Φc. The range of the CB content in which the sample has an obvious PTC effect depends on the crystallinity of the matrix. The increase in the crystallinity will broaden this range. When Φ is situated between Φpc and Φc, the air-cooled samples have small PTC intensities, which are caused by the high room-temperature resistivities (shown in Fig. 2).

Figure 5 shows the relations among PTC, NTC intensities, and the degree of the crystallinity of the sample of PVDF/0.11 CSF3. These two intensities both increase as the crystallinity increases. It is probable that high crystallinity brings a large volume expansion of the matrix. More conductive pathways are broken down when the crystalline regions are melting. Above the melting point, more energy is added to the CBs; then the flocculation of the CBs and phase separation of the composite become easier.[23]

CONCLUSION

Φpc and Φc decrease, and PTC and NTC intensities increase, as the crystallinity increases. T_c and T_m shift to low temperature due to the imperfection and the small size of the crystallites of the crystalline polymer. The width of the ρ–T curve depends on the distribution of the size and the degree of the perfection of crystallites.

All the results give new evidence in favor of the model that CBs distribute in amorphous regions around the crystalline regions within the crystalline polymer matrix. The CBs, in general, are in a thermodynamically nonequilibrium state, especially at the melting temperature. The expansion of the crystalline regions caused the PTC effect. The high energies of the CBs and the low shear modulus of the matrix are the main reasons for the NTC effect.

REFERENCES

1. J. Gurland, *Trans. Met. Soc. AIME*, **236**, 642 (1966).
2. S. M. Aharoni, *J. Appl. Phys.*, **43**, 2463 (1972).
3. F. Bueche, *J. Appl. Phys.*, **43**, 4837 (1972).
4. B. E. Springett, *J. Appl. Phys.*, **44**, 2925 (1973).
5. A. H. Trivedi, J. Garcia, A. B. Burhan, and D. L. Schruben, *Polym. Eng. Sci.*, **34**, 1115 (1994).
6. A. M. Lyons, *Polym. Eng. Sci.*, **31**, 445 (1991).
7. K. Ohe and Natio, *Jpn. J. Appl. Phys.*, **10**, 99 (1971).
8. J. Meyer, *Polym. Eng. Sci.*, **13**, 462 (1973).
9. M. Narkis, A. Ram, and F. Flashner, *J. Appl. Polym. Sci.*, **22**, 163 (1978); *Polym. Eng. Sci.*, **18**, 649 (1978).
10. T. Asada, *Int. Polym. Sci. Technol.*, **14**, 25 (1987).
11. H. Tang, J. H. Piao, X. F. Chen, Y. X. Luo, and S. H. Li, *J. Appl. Polym. Sci.*, **48**, 1795 (1993).
12. W. T. Jia and X. F. Chen, *J. Appl. Polym. Sci.*, **54**, 1219 (1994).
13. F. Bueche, *J. Appl. Phys.*, **44**, 532 (1973).
14. F. Kohler, U.S. Pat. 3,234,753, (March 29, 1966).
15. K. Miyasaka, K. Watanabe, E. Jojima, H. Aida, M. Sumita, and K. Ishikawa, *J. Mater. Sci.*, **17**, 1610 (1982).
16. M. Sumita, H. Abe, H. Kayaki, and K. Miyasaka, *J. Macromol. Sci.-Phys. B*, **25**(1, 2), 171 (1986).
17. A. K. Sircar and J. L. Wells, *Polym. Eng. Sci.*, **21**, 809 (1981).
18. J. Meyer, *Polym. Eng. Sci.*, **14**, 706 (1974).
19. Nakagawa and Ishida, 1973.
20. A. I. Medalia, *Rubb. Chem. Technol.*, **59**, 432 (1985).
21. F. Bueche, *Physical Properties of Polymers*, Interscience, New York, 1962, pp. 309–310.
22. B. Wessling, *Polym. Eng. Sci.*, **31**, 1200 (1991).
23. M. Narkis, A. Ram, and Z. Stein, *Polym. Eng. Sci.*, **21**, 1049 (1981).

Received September 21, 1995
Accepted April 19, 1996